

## $L\gamma_1$ and $L\beta_{2,15}$ x-ray emission lines of rare-earth trifluorides and $CeO_2$

This article has been downloaded from IOPscience. Please scroll down to see the full text article.

1997 J. Phys.: Condens. Matter 9 10789

(<http://iopscience.iop.org/0953-8984/9/48/020>)

View [the table of contents for this issue](#), or go to the [journal homepage](#) for more

Download details:

IP Address: 171.66.16.209

The article was downloaded on 14/05/2010 at 11:44

Please note that [terms and conditions apply](#).

## $L\gamma_1$ and $L\beta_{2,15}$ x-ray emission lines of rare-earth trifluorides and $\text{CeO}_2$

K Jouda†§, S Tanaka‡ and O Aita†||

† College of Engineering, Osaka Prefecture University, Gakuen-cho 1, Sakai, Osaka 599-8531, Japan

‡ College of Integrated Arts and Sciences, Osaka Prefecture University, Gakuen-cho 1, Sakai, Osaka 599-8531, Japan

Received 30 June 1997

**Abstract.** X-ray emission spectra due to the rare-earth  $4d \rightarrow 2p_{1/2}$  ( $L\gamma_1$ ) and  $4d \rightarrow 2p_{3/2}$  ( $L\beta_{2,15}$ ) electronic transitions in rare-earth compounds have been measured with x-ray excitation. The satellite structure due to the 4d–4f exchange interaction in the final state is observed in Ce compounds, as seen in other heavier rare-earth compounds. The intensity ratio of the satellite to the main band in the  $L\gamma_1$  line is larger than that in the  $L\beta_{2,15}$  line, which is conspicuous in heavy rare-earth compounds. The experimental results are well explained by the theoretical calculation, where the multiplet couplings and the dependence of the 4d core-hole decay rate on the multiplet terms are taken into account. It is found that the spectral shapes of  $\text{CeF}_3$  and  $\text{CeO}_2$  resemble each other as a result of the phase matching of the wave functions between the intermediate and final states.

### 1. Introduction

Core-level spectroscopies, such as x-ray photoemission, x-ray absorption and x-ray emission spectroscopies, play an important role in investigating the electronic states in the strongly correlated systems [1]. In these spectroscopies, the many-body effect is very important for interpreting the spectral features. It is well known that the characteristic x-rays of  $L\gamma_1$  and  $L\beta_{2,15}$  lines in rare-earth compounds, which are attributed to the  $4d \rightarrow 2p_{1/2}$  and  $4d \rightarrow 2p_{3/2}$  dipole transitions, respectively, have a satellite structure due to the strong exchange interaction between a 4d core hole and a 4f electron. It is more than two decades ago that these satellite structures in all of the oxides of rare-earth metals except for La and Pm were observed by Demekhin *et al* with high-energy electron beam excitation [2]. They found that the energy separation between the satellite and the main band increases from Pr to Gd, and then decreases from Gd to Yb. They interpreted this tendency on the basis of the value of the 4f spin angular momentum of these compounds. Although the energy separation between the main band and the satellite seems to correlate with the 4f spin angular momentum, the spectral profiles cannot be precisely reproduced by this interpretation. This implies that the contribution of the orbital angular momentum is also very important in the final state of the  $4d \rightarrow 2p$  x-ray emission process.

§ Deceased.

|| Author to whom any correspondence should be addressed: telephone: +81-722-52-1161 (extension 2392); fax: +81-722-59-3340; e-mail: aita@sp.ms.osakafu-u.ac.jp

Recently, Tanaka *et al* calculated the  $4d \rightarrow 2p$  x-ray emission spectra (XES) of  $\text{Ce}_2\text{O}_3$ ,  $\text{Pr}_2\text{O}_3$  and  $\text{Dy}_2\text{O}_3$  with the Anderson impurity model by taking account of the multiplet couplings, where the x-ray emission process from excitation to emission is treated as a coherent second-order optical process [3]. They found that the calculated results for  $\text{Pr}_2\text{O}_3$  and  $\text{Dy}_2\text{O}_3$  reproduce the experimental results well. They also clarified that the  $4d$  spin-orbit interaction in the final state and the  $4f$  spin-orbit interaction in the initial state are responsible for the general trend for the intensity ratio of the satellite to the main band (the branching ratio) in the  $L\gamma_1$  lines to be larger than that in the  $L\beta_{2,15}$  lines.

In addition, the decay mechanism of the  $4d$  core hole has a great influence on the  $4d \rightarrow 2p$  XES. In heavy rare-earth elements, the  $4d$  core-hole state decays mainly by the  $4d-4f4f$  super-Coster-Kronig (s-CK) Auger process. The s-CK Auger decay rate strongly depends upon the multiplet terms of the  $4d$  core-hole state: the decay rate of the low-spin state in the  $4d$  core-hole state is larger than that of the high-spin state, because of the spin selection rule in the Auger transition. The term dependence of the s-CK Auger decay rate was first discovered by Ogasawara *et al* in the analysis of  $4d$  x-ray photoemission spectra (XPS) of the rare-earth oxides [4]. Since the final state in the  $4d \rightarrow 2p$  XES coincides with that of the  $4d$  XPS, it is necessary to consider the term dependence of the decay rate of the  $4d$  core hole in the final state of the  $4d \rightarrow 2p$  x-ray emission process. Tanaka *et al* illustrated the importance of this effect on the  $4d \rightarrow 2p$  XES by calculating the  $4d \rightarrow 2p$  XES in  $\text{Dy}_2\text{O}_3$  [3].

While the multiplet coupling is important in the heavy rare-earth compounds, the hybridization effect tends to be more important in the light rare-earth compounds. In this connection, over ten years ago Tsutsumi *et al* investigated experimentally the  $4d \rightarrow 2p$  XES of the various valence systems of Sm, such as Sm metal,  $\text{Sm}_2\text{O}_3$ ,  $\text{SmB}_6$ , SmS and SmSe [5]. However, they did not find any significant difference in the spectral shapes among them. Tanaka *et al* clarified that the hybridization effect on the XES of  $\text{Ce}_2\text{O}_3$  and  $\text{Pr}_2\text{O}_3$  is smeared out, when the x-ray emission takes place between the core levels of the rare-earth elements [3]. In this case, the effects of the core potential on the valence states are nearly the same in the intermediate and in the final states, so the wave functions of the valence states are not so changed from the intermediate to the final states. Therefore, any distinct structure due to the electronic charge redistribution from the intermediate to the final states does not appear, which is what we called the *phase matching* of the wave functions between the intermediate and the final states.

The main purpose here is to measure the  $L\gamma_1$  and the  $L\beta_{2,15}$  lines of the rare-earth compounds precisely in order to compare them with the recently calculated results of Tanaka *et al*. To this end, we use the high-energy x-rays from a tungsten target as an incident excitation source, by which means we can avoid the various complicated scattering processes caused by the electron beam excitation. We investigate the  $4d \rightarrow 2p$  XES of  $\text{LaF}_3$ ,  $\text{CeF}_3$ ,  $\text{PrF}_3$ ,  $\text{GdF}_3$ ,  $\text{TbF}_3$  and  $\text{DyF}_3$ , which are chemically stable, rather than the oxides. We also investigate the  $4d \rightarrow 2p$  XES of  $\text{CeO}_2$ , which is a typical example of a strong-valence-mixing system and a good testing material for studying the hybridization effect on the  $4d \rightarrow 2p$  XES.

## 2. Experimental procedure

The measurements of the  $4d \rightarrow 2p$  XES were carried out with a double-crystal spectrometer, where the (101) planes of quartz crystals were used in the (1, +1) position. The full width at half-maximum (FWHM) of the (1, -1) rocking curve was from 0.53 eV in the wavelength region of the La  $L\gamma_1$  emission to 0.89 eV in the Dy  $L\gamma_1$  region. An x-ray tube with a

tungsten target was operated at 47.5 keV and 33 mA as a primary x-ray source. Fluorescent x-rays were detected by a gas-flow proportional counter with P-10 gas (90% argon and 10% methane). Samples were prepared by pressing fine powder into pellets. All of the specimens were kept in an evacuated sample chamber. Intensity measurements were carried out automatically for a preset counting time at regular intervals of  $0.001\ 25^\circ$  of the Bragg angle. Appropriate lines of  $K\alpha_{1,2}$  and  $K\beta_{1,3}$  emissions of transition metals were used as the reference lines for the measurement of each of the rare-earth  $L\gamma_1$  and  $L\beta_{2,15}$  lines, and their wavelengths were taken from a table [6]. During the measurements the temperature of the spectrometer and the counter was stabilized within  $\pm 1.5^\circ C$ .

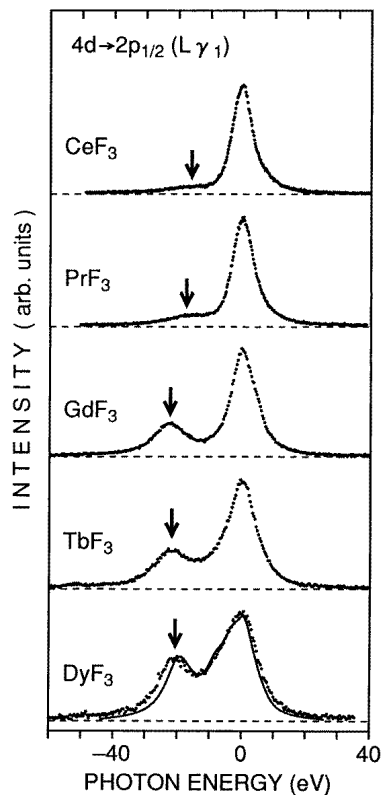


**Figure 1.** Experimental results for the  $4d \rightarrow 2p_{1/2}$  ( $L\gamma_1$ ) XES of  $CeF_3$ ,  $PrF_3$ ,  $GdF_3$ ,  $TbF_3$  and  $DyF_3$ . The calculated result for the  $L\gamma_1$  line for the  $Dy^{3+}$  ion [3] is also shown, by the solid line.

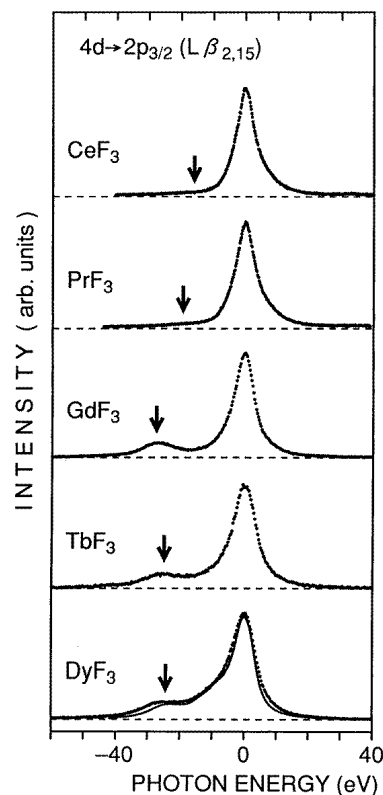


**Figure 2.** Experimental results for the  $4d \rightarrow 2p_{3/2}$  ( $L\beta_{2,15}$ ) XES of  $CeF_3$ ,  $PrF_3$ ,  $GdF_3$ ,  $TbF_3$  and  $DyF_3$ . The calculated result for the  $L\beta_{2,15}$  line for the  $Dy^{3+}$  ion [3] is also shown, by the solid line.

### 3. Results and discussion

Experimental results for the  $4d \rightarrow 2p_{1/2}$  ( $L\gamma_1$ ) and  $4d \rightarrow 2p_{3/2}$  ( $L\beta_{2,15}$ ) XES of  $CeF_3$ ,  $PrF_3$ ,  $GdF_3$ ,  $TbF_3$  and  $DyF_3$  are shown in figures 1 and 2, respectively. The origin of the abscissa is taken at the energy position of the main peak for each spectrum. Each of these spectra has a main band with a satellite, indicated by an arrow in the figure, on the low-energy side of the main band. The branching ratio of the heavy rare-earth compounds is larger than that of

the light rare-earth compounds. In addition, we can see the general trend for the branching ratio in the  $L\gamma_1$  line to be larger than that in the  $L\beta_{2,15}$  line for these compounds. Though these spectral features are similar to the previous results obtained by Demekhin *et al* [2], our results are slightly different from them in the spectral shapes and the branching ratios: for example, the branching ratio in the  $L\gamma_1$  line of Pr in the present results is half the size of the result obtained by Demekhin *et al*. In particular, we observed the satellite structure in Ce compounds for the first time.

The satellite structure is mainly attributed to the 4d–4f exchange interaction in the final state of the  $4d \rightarrow 2p$  x-ray emission, and the satellite corresponds to the low-spin final state, where the spins of 4f and 4d electrons are antiparallel to each other. If we neglect the orbital angular momentum of the 4f state, the branching ratio is represented by the statistical ratio  $S/(S+1)$ , where  $S$  stands for the 4f spin angular momentum in the initial state. Then, the branching ratio in  $GdF_3$  would be the largest among all of those of these compounds, because  $GdF_3$  has the largest value of the 4f spin angular momentum according to Hund's rule. However, as seen in figures 1 and 2, the branching ratio in  $GdF_3$  is smaller than that in  $DyF_3$ , and the branching ratio for each compound substantially differs from the ratio  $S/(S+1)$ .

Recently, Tanaka *et al* calculated the  $4d \rightarrow 2p$  XES of rare-earth compounds with the Anderson impurity model by taking account of the multiplet couplings [3]. Their results for the  $L\gamma_1$  and  $L\beta_{2,15}$  lines for a free  $Dy^{3+}$  ion, which are the only results available calculated for the free ion, are shown in figures 1 and 2, respectively, by solid lines. In the calculation, the term dependence of the 4d core-hole decay is also taken into account. The calculated results are in good agreement with our experimental results, even though the solid-state effect is completely neglected in the calculation.

Tanaka *et al* concluded that some of the high- (low-) spin components merge into the satellite (main band) through the multiplet couplings. As a result, the branching ratio deviates from the ratio  $S/(S+1)$ . Furthermore, a good correspondence between the experiments and the calculation suggests that the estimation of the term dependence of the 4d core-hole decay rate [4] is also supported by the  $4d \rightarrow 2p$  XES.

Next, in order to investigate the hybridization effect on the  $4d \rightarrow 2p$  XES, we show the experimental results for  $LaF_3$ ,  $CeF_3$  and  $CeO_2$ . Experimental results for the  $4d \rightarrow 2p_{1/2}$  ( $L\gamma_1$ ) and  $4d \rightarrow 2p_{3/2}$  ( $L\beta_{2,15}$ ) XES of  $CeF_3$ ,  $CeO_2$  and  $LaF_3$  are shown in figures 3 and 4, respectively. The origin of the abscissa is taken at the energy position of the main peak. For these compounds, we have commonly obtained a broad single peak with a tail extending toward the high-energy side. The FWHM of the main band of the  $L\gamma_1$  ( $L\beta_{2,15}$ ) line is 7.5 (7.1), 7.1 (6.9) and 5.1 (4.9) eV for  $CeF_3$ ,  $CeO_2$  and  $LaF_3$ , respectively. In the  $L\gamma_1$  line of  $CeF_3$ , a broad and weak satellite structure appears around  $-16$  eV, and in the  $L\gamma_1$  line of  $CeO_2$  there is some intensity around  $-16$  eV, but we can hardly see any structure in this region of the  $L\gamma_1$  line of  $LaF_3$ .

It should be noted that the overall spectral features of these compounds look very similar to each other. These results are strikingly in contrast to the spectral features of the 4d XPS: the spectral features of these compounds are very different from each other [7, 8]. The core-level XPS, such as the 3d and 4d XPS, for these compounds strongly reflect the effect of hybridization between the 4f and the valence states [9–11]:  $CeO_2$  has a well-known three-peak structure in 3d and 4d XPS, while  $CeF_3$  has a two-peak structure.

Since the final state in the  $4d \rightarrow 2p$  XES is just the same as that in the 4d XPS, it may be expected that the spectral shape of the  $4d \rightarrow 2p$  XES for  $CeO_2$  will become quite different from that for  $CeF_3$ . However, a similarity in the shape of the  $4d \rightarrow 2p$  XES between  $CeO_2$  and  $CeF_3$  suggests that the hybridization effect contributes to a second-order

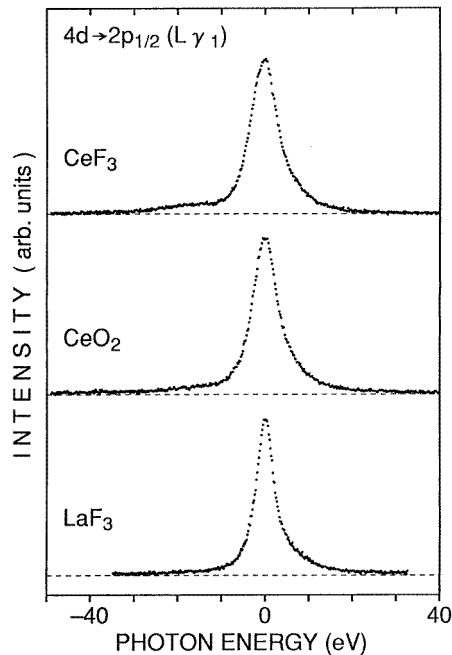


**Figure 3.** Experimental results for the  $4d \rightarrow 2p_{1/2}$  ( $L\gamma_1$ ) XES of  $CeF_3$ ,  $CeO_2$  and  $LaF_3$ .

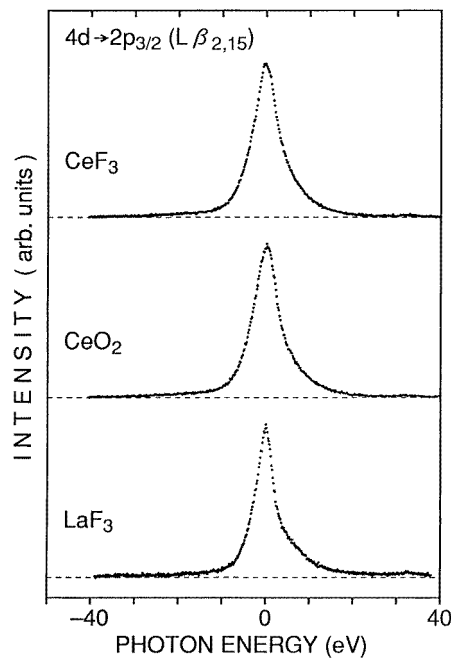


**Figure 4.** Experimental results for the  $4d \rightarrow 2p_{3/2}$  ( $L\beta_{2,15}$ ) XES of  $CeF_3$ ,  $CeO_2$  and  $LaF_3$ .

optical process in a very different manner compared with a first-order optical process; that is, the intermediate state plays an important role in the x-ray emission process.

In the  $4d \rightarrow 2p$  XES,  $2p$  and  $4d$  core-hole potentials act on the  $4f$  level in the intermediate and final states, respectively. When the two core-hole potentials are almost the same, the effects of hybridization between the  $4f$  level and the valence band become nearly equal for the intermediate and the final states. In this situation, the systems composed of the  $4f$  and the valence states are described by the same Hamiltonian in the intermediate and final states with the exception of multiplet effects. Hence, because of the phase matching of the wave functions between the intermediate and final states, the transition probability of the cross transition, which means the transition from one of the intermediate states to a different final eigenstate, completely vanishes. The value of the  $2p$  core-hole potential is not known exactly as yet, but it is estimated to be about the same as the  $3d$  core-hole potential, which is a little larger than the  $4d$  core-hole potential [3]. Thus, our result is experimental evidence that the phase-matching effect almost smears out the hybridization effect in the  $4d \rightarrow 2p$  XES. As a result, the overall spectral features of the  $4d \rightarrow 2p$  XES of  $CeF_3$  and  $CeO_2$  look very similar. We can see that the FWHM and the intensity of the satellite are slightly different for  $CeF_3$  and  $CeO_2$ . This is possibly because the condition of complete phase matching is not fulfilled by the multiplet couplings, and because of the difference between the core-hole potentials of the intermediate and final states.

In  $LaF_3$ , although there are almost no  $4f$  electrons in the ground state, a small occupation of the  $4f$  state is brought about by the hybridization in the intermediate and final states. Therefore, the asymmetry in the shape of the main band is considered to be due to the multiplet coupling between the  $4f$  electron and a  $4d$  core hole in the final state. However, the occupation of the  $4f$  state is too small for one to see the satellite.

#### 4. Conclusion

In this work, we have obtained the  $4d \rightarrow 2p$  XES of  $\text{LaF}_3$ ,  $\text{CeF}_3$ ,  $\text{PrF}_3$ ,  $\text{GdF}_3$ ,  $\text{TbF}_3$ ,  $\text{DyF}_3$  and  $\text{CeO}_2$  under x-ray excitation. The satellite structure due to the  $4d$ - $4f$  exchange interaction in the final state was observed for the first time in Ce compounds. In each compound, the branching ratio in the  $L\gamma_1$  line is larger than that in the  $L\beta_{2,15}$  line, which is consistent with the theoretical analysis. A good agreement between the experimental and the calculated results supports the multiplet term dependence of the  $4d$  core-hole decay rate in the  $4d \rightarrow 2p$  XES of heavy rare earths pointed out by Ogasawara *et al* [4]. It is found that the spectral features of the  $4d \rightarrow 2p$  XES of  $\text{CeO}_2$  are very similar to those for  $\text{CeF}_3$ , which is quite a contrast to the case for the core-level XPS in these compounds. From these results, we conclude that the  $2p$  core-hole potential is nearly the same as the  $3d$  core-hole potential.

#### Acknowledgments

The authors would like to thank Professor K Ichikawa and Dr Y Taguchi for valuable discussions. One of the authors (ST) thanks Professor A Kotani and Dr H Ogasawara for stimulating discussions and valuable comments.

#### References

- [1] Kotani A 1988 *Core-Level Spectroscopy in Condensed Systems* ed J Kanamori and A Kotani (Berlin: Springer) p 3
- [2] Demekhin V F, Platkov A I and Lyubivaya M V 1972 *Sov. Phys.-JETP* **35** 28
- [3] Tanaka S, Ogasawara H, Okada K and Kotani A 1995 *J. Phys. Soc. Japan* **64** 2225
- [4] Ogasawara H, Kotani A and Thole B T 1994 *Phys. Rev. B* **50** 12332
- [5] Tsutsumi K, Aita O and Watanabe T 1982 *Phys. Rev. B* **25** 5415
- [6] Bearden J A 1967 *Rev. Mod. Phys.* **39** 78
- [7] Suzuki S, Ishii T and Sagawa T 1974 *J. Phys. Soc. Japan* **37** 1334
- [8] Burroughs P, Hamnett A, Orchard A F and Thornton G 1976 *J. Chem. Soc. Dalton Trans.* **17** 1686
- [9] Jo T and Kotani A 1988 *J. Phys. Soc. Japan* **57** 2288
- [10] Imada S and Jo T 1989 *J. Phys. Soc. Japan* **58** 2665
- [11] Kotani A and Ogasawara H 1992 *J. Electron Spectrosc. Relat. Phenom.* **60** 257 and references cited therein